COMPDYN 2011
III ECCOMAS Thematic Conference on
Computational Methods in Structural Dynamics and Earthquake Engineering
M. Papadrakakis, M. Fragiadakis, V. Plevris (eds.)
Corfu, Greece, 25–28 May 2011

AN EFFICIENT QUADRATURE BEAM MODEL TO SIMULATE INELASTIC SEISMIC BEHAVIOR OF STEEL FRAMES

R. He[1], R. Zhang[1], and H. Zhong[1]

[1] Department of Civil Engineering, Tsinghua University
Beijing 100084, China
e-mail: ruihe@tsinghua.edu.cn

Keywords: Distributed Plasticity, Consistent Mass Matrix, Seismic Time History Analysis, Quadrature Beam Model, Force-based Beam Model.

Abstract. *Developing nonlinear structural models with high accuracy and affordable computing cost is a challenging issue and one of the pressing needs in earthquake engineering. The paper presents a quadrature beam model for distributed plasticity seismic analysis of steel frames. It is based on the newly developed weak-form quadrature element method, in which the variation principle and the differential quadrature analog are combined. One quadrature beam element can simulate a beam-column member with varying cross-section and non-uniformly distributed loads. The formulations of tangent stiffness matrix and consistent mass matrix are derived. The section constitutive relation of a beam-column member is directly derived using fiber model and material properties. Inelastic time history analysis of the LA 3-story moment-resisting steel frame is conducted to demonstrate the accuracy and efficiency of the quadrature beam model. For verification and comparison, the frame is also analyzed using ANSYS with its BEAM188 element and OpenSEES with the force-based beam element. It is shown that: a) by increasing the number of integration points in one element, results of the quadrature beam model are in excellent agreement with those computed by the displacement-based model in ANSYS; b) degrees of the freedom and the CPU time consumption of the quadrature beam model are much lower than those of the displacement-based model; c) the convergence rate of the quadrature beam model is comparable to that of the force-based model, and the time consumption of the quadrature beam model is slightly higher. In contrast to the only available lumped mass matrix of the force-based model, it is easy to acquire consistent mass matrix in the quadrature beam model for inelastic dynamic analysis, highlighting its great potentials in seismic analysis of frames.*

1 INTRODUCTION

Developing nonlinear structural models with high accuracy and affordable computing cost is a challenging issue and one of the pressing needs in earthquake engineering [1]. For inelastic seismic analysis of frame structures, the lumped plasticity model [2] enjoys simplicity and computational efficiency but it cannot simulate the spread of plasticity and its empirical designation of hinge positions and spring properties sometimes leads to unreliable results. The distributed plasticity model is usually regarded to be more accurate.

One way to construct a distributed plasticity model is using displacement-based (DB) finite beam elements. Elements based on cubic [3] and quartic [4] shape functions were previously studied. These elements with only a few internal nodes are insufficient to carry out seismic analysis of frames with one element per member. When using a higher-order nodal element, the whole set of shape functions has to be reformulated when increasing the order and the simple choice of nodal points may yield ill-condition stiffness matrices [5]. The research work extending the p-version element to inelastic analysis of frames has been rather sparse yet.

Another way is using a force-based (FB) beam element, which adopts exact interpolation functions for internal forces and avoids discretization errors accordingly [6-8]. It realizes simulation of a nonlinear frame member with one beam element, leading to lower DOFs. The FB element prevails in earthquake engineering platform OpenSEES [6] for seismic analysis of frames. However, implementation of FB elements in a finite element program suffers some inconvenient procedures when dealing with non-uniformly distributed loads, state determination [7-8], geometrical nonlinearity [9] and consistent mass matrices [10], etc.

In this paper, a new distributed plasticity model, named as quadrature beam (QB) model, is presented for seismic analysis of structures. It is based on the newly developed weak-form quadrature element method, in which the variation principle and the differential quadrature analog are combined. The weak-form quadrature element method has been validated to be accurate and efficient in elastic problems of varying cross sections [11-12]. In this paper, a distributed plasticity QB beam model is formulated. Its consistent mass matrix is given for dynamic analysis. Inelastic time history analysis of the LA 3-story steel frame [13] is conducted as an example. The accuracy, convergence and CPU time consumption of the QB model are evaluated, and compared with those of the DB and FB models. Results indicate that the quadrature beam model is accurate and efficient.

2 DIFFERENTIAL QUADRATURE ANALOGS

The essence of the conventional differential quadrature analog is that the derivative of a function at a grid point is expressed by weighted linear summation of function values at all grid points in the domain of problem [14]. For instance, the first order derivative of a function f with respect to a variable ξ at a grid point $\xi = \xi_i$ is approximated by

$$\left.\frac{\mathrm{d}f}{\mathrm{d}\xi}\right|_{\xi=\xi_i} = \sum_{j=1}^{M} C_{ij}^{(1)} f(\xi_j),\ i = 1, 2, \cdots, M \tag{1}$$

where $C_{ij}^{(1)}$ are the weighting coefficients for first order derivatives, which are only dependent upon the number of grid points M and their explicit expressions are given by [12]

$$C_{ij}^{(1)}=\begin{cases}\dfrac{g'(\xi_i)}{(\xi_i-\xi_j)g'(\xi_j)}, & i\neq j;\\ -\displaystyle\sum_{k=1,k\neq i}^{M} C_{ik}{}^{(1)}, & i=j;\end{cases} \qquad g(\xi)=\prod_{j=1}^{M}(\xi-\xi_j) \tag{2}$$

For Bernoulli-Euler beam analysis, the C1 continuity at ends of the element requires generalized differential quadrature analogs where the first order derivative of the function at each end is included in approximation. Thus, the *n*th order derivatives is approximated by

$$\left.\frac{\mathrm{d}^n f}{\mathrm{d}\xi^n}\right|_{\xi=\xi_i}=G_{i1}^{(n)}\left.\frac{\mathrm{d}f}{\mathrm{d}\xi}\right|_{\xi=\xi_1}+\sum_{j=1}^{M}G_{i(j+1)}^{(n)}f(\xi_j)+G_{i(M+2)}^{(n)}\left.\frac{\mathrm{d}f}{\mathrm{d}\xi}\right|_{\xi=\xi_M} \tag{3}$$

where $G_{ij}^{(n)}$ are the weighting coefficients which can be determined by Hermitian interpolation functions, i.e.

$$G_{i1}^{(n)}=h_{11}^{(n)}(\xi_i),\quad G_{i(M+2)}^{(n)}=h_{M1}^{(n)}(\xi_i),\quad G_{i(j+1)}^{(n)}=h_{j0}^{(n)}(\xi_i),\quad j=1,2,\cdots,M \tag{4}$$

where Hermitian interpolation functions are given by

$$\begin{aligned}
h_{11}(\xi)&=\frac{(\xi-\xi_1)(\xi-\xi_M)}{\xi_1-\xi_M}l_1(\xi),\\
h_{M1}(\xi)&=\frac{(\xi-\xi_1)(\xi-\xi_M)}{\xi_1-\xi_M}l_M(\xi),\\
h_{10}(\xi)&=\frac{\xi-\xi_M}{\xi_1-\xi_M}[1-(\xi-\xi_1)(l_1'(\xi_1)+\frac{1}{\xi_1-\xi_M})]l_1(\xi),\\
h_{M0}(\xi)&=\frac{\xi-\xi_1}{\xi_M-\xi_1}[1-(\xi-\xi_M)(l_M'(\xi_M)+\frac{1}{\xi_M-\xi_1})]l_M(\xi),\\
h_{j0}(\xi)&=\frac{(\xi-\xi_1)(\xi-\xi_M)}{(\xi_j-\xi_1)(\xi_j-\xi_M)}l_j(\xi),\quad j=2,3,\cdots,M-1
\end{aligned} \tag{5}$$

with

$$l_j(\xi)=\frac{g(\xi)}{(\xi-\xi_j)g'(\xi_j)} \tag{6}$$

Differential quadrature analogs are characterized by that only the function values and derivatives at grid points are concerned, so approximation of derivatives is direct and efficient.

3 FORMULATION OF THE QUADRATURE BEAM MODEL

3.1 Model and assumptions

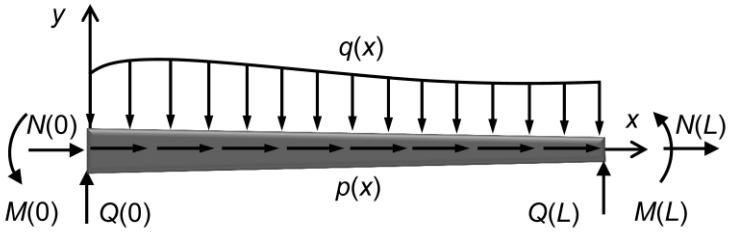

Figure 1: A planar beam model with varying cross-section

A planar beam model with varying cross section is shown in Figure 1. The Bernoulli-Euler beam theory and the hypothesis of plane section hold true. Small deflections and moderate rotation are assumed. The transverse shear deformations are not considered here. In Figure 1, (x, y) is the local coordinate system attached to the beam where x is in the axial direction. L is the beam length. N and Q are axial and shear forces at beam ends, and M is concentrated moments. p and q are non-uniform distributed loads in the x and y directions, respectively. u and v are the translational displacement components along x and y directions, respectively.

For a Bernoulli-Euler beam, the deformations at a certain section x are usually represented by the axial strain at the reference axis ε_x and curvatures κ. And the corresponding section forces are the axial load N and the bending moment M. Generally the section deformation is given in terms of the displacements as

$$\boldsymbol{\varepsilon}(x)=\begin{Bmatrix}\varepsilon_x\\ \kappa\end{Bmatrix}=\begin{Bmatrix}\dfrac{\mathrm{d}u}{\mathrm{d}x}\\ \dfrac{\mathrm{d}^2v}{\mathrm{d}x^2}\end{Bmatrix} \tag{7}$$

For nonlinear problems, an incremental section constitutive relation is usually written, i.e.

$$\delta\mathbf{R}(x)=\mathbf{k}(x)\delta\boldsymbol{\varepsilon}(x) \tag{8}$$

where $\mathbf{R}(x) = [N \;\; M]^{\mathrm{T}}$ is the vector of internal forces at section x. $\mathbf{k}(x)$ is the section stiffness matrix given by

$$\mathbf{k}(x)=\begin{bmatrix}k_{11} & k_{12}\\ k_{21} & k_{22}\end{bmatrix} \tag{9}$$

Once the section deformation $\boldsymbol{\varepsilon}(x)$ is known, the internal forces $\mathbf{R}(x)$ and section stiffness matrix $\mathbf{k}(x)$ can be obtained using either fiber section models or load-deformation relations of sections. Details of inelastic section models can be found in [4] and [8]. Different models at sections in one member can be used to deal with problems of varying cross sections and even varying material properties.

3.2 Variation principles and static equilibrium equations

Inducing a dimensionless coordinate $\xi = 2x/L\text{-}1$, the governing equations of the above problem are established from virtual work principle, i.e.

$$\delta U_{\text{int}}^{(\text{e})} + \delta U_{\text{ext}}^{(\text{e})} = 0 \tag{10}$$

where the internal virtual work and the external virtual work are given by

$$\begin{aligned} \delta U_{\text{int}}^{(\text{e})} &= S\int_{-1}^{1} \delta\bar{\boldsymbol{\varepsilon}}^{\text{T}}\mathbf{R}\,\text{d}\xi \\ \delta U_{\text{ext}}^{(\text{e})} &= -S\int_{-1}^{1}\left(p\delta u + q\delta v\right)\text{d}\xi - (N\delta u + Q\delta v + \frac{M}{S}\frac{\text{d}v}{\text{d}\xi})\Big|_{\xi=-1} - (N\delta u + Q\delta v + \frac{M}{S}\frac{\text{d}v}{\text{d}\xi})\Big|_{\xi=+1} \end{aligned} \tag{11}$$

and $S = L/2$. Lobatto integration rule with M sampling points (see Fig. 2) is used to evaluate the integrals, resulting in

$$S\sum_{i=1}^{M} W_i \delta\bar{\boldsymbol{\varepsilon}}_i^{\text{T}}\mathbf{R}_i = \delta\mathbf{d}^{(\text{e})\text{T}}\mathbf{F}^{(\text{e})} \tag{12}$$

where $\boldsymbol{\varepsilon}_i = \boldsymbol{\varepsilon}(\xi_i)$, $\mathbf{R}_i = \mathbf{R}(\xi_i)$, ξ_i and W_i are the Lobatto sampling points and weighting coefficients [15]. The element nodal displacement vector in Eq. (12) is written as

$$\mathbf{d}^{(\text{e})} = \begin{bmatrix} \mathbf{d}_1^{\text{T}} & \mathbf{d}_M^{\text{T}} & \mathbf{d}_2^{\text{T}} & \cdots & \mathbf{d}_{M-1}^{\text{T}} \end{bmatrix}^{\text{T}} \tag{13}$$

where

$$\mathbf{d}_i^{\text{T}} = \begin{cases} \begin{bmatrix} u_i & v_i & \left(\dfrac{\text{d}v}{\text{d}\xi}\right)_i \end{bmatrix}, & i = 1, M; \\ \begin{bmatrix} u_i & v_i \end{bmatrix}, & i = 2, \ldots, M\text{-}1. \end{cases} \tag{14}$$

Correspondingly, the element nodal force vector in Eq. (12) is expressed by

$$\mathbf{F}^{(\text{e})} = \begin{bmatrix} \mathbf{F}_1^{\text{T}} & \mathbf{F}_M^{\text{T}} & \mathbf{F}_2^{\text{T}} & \cdots & \mathbf{F}_{M-1}^{\text{T}} \end{bmatrix}^{\text{T}} \tag{15}$$

where

$$\mathbf{F}_i^{T} = \begin{cases} \begin{bmatrix} N(\xi_i) + SW_i p(\xi_i) & Q(\xi_i) + SW_i q(\xi_i) & M(\xi_i)/S \end{bmatrix}, & i = 1, M; \\ \begin{bmatrix} SW_i p(\xi_i) & SW_i q(\xi_i) \end{bmatrix}, & i = 2, \ldots, M. \end{cases} \tag{16}$$

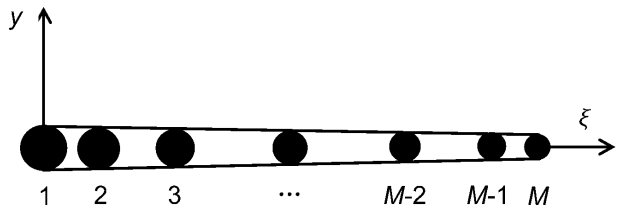

Figure 2: Lobatto points of a QB element

Based on differential quadrature analogs, the derivatives in section deformation vectors at the Lobatto points $\boldsymbol{\varepsilon}_i$ are directly approximated using the nodal displacement vector $\mathbf{d}^{(\text{e})}$. The section deformation vector at Lobatto points i is expressed in terms of ξ coordinate as

$$\boldsymbol{\varepsilon}_i = \mathbf{D}\boldsymbol{\varepsilon}_{0i} \tag{17}$$

where $\mathbf{D}=\mathrm{diag}\left[1/S \quad 1/S^2 \quad 1/S^2\right]$ and

$$\begin{aligned}
&\boldsymbol{\varepsilon}_{0i}=\left[\left(\frac{\mathrm{d}u}{\mathrm{d}\xi}\right)_i \quad \left(\frac{\mathrm{d}^2v}{\mathrm{d}\xi^2}\right)_i\right]^{\mathrm{T}}=\mathbf{B}_{0i}\mathbf{d}^{(\mathrm{e})}, \quad (i=1,\cdots,M);\\
&\mathbf{B}_{0i}=\left[\mathbf{B}_{0i,2} \quad \tilde{\mathbf{B}}_{0i,1} \quad \mathbf{B}_{0i,M+1} \quad \tilde{\mathbf{B}}_{0i,M+2} \quad \mathbf{B}_{0i,3} \quad \cdots \quad \mathbf{B}_{0i,M}\right]\\
&\mathbf{B}_{0i,j}=\begin{bmatrix} C_{i(j-1)}^{(1)} & 0 \\ 0 & G_{ij}^{(2)} \end{bmatrix}, \tilde{\mathbf{B}}_{0i,j}=\begin{bmatrix} 0 & 0 \\ 0 & G_{ij}^{(2)} \end{bmatrix}
\end{aligned} \tag{18}$$

After substitution of the section deformation approximation in Eqs. (17-18) into Eq. (12), the incremental-form equilibrium equations are obtained as

$$\delta\mathbf{F}^{(\mathrm{e})}=\mathbf{K}^{(\mathrm{e})}\delta\mathbf{d}^{(e)} \tag{19}$$

where the element tangent stiffness matrix is given by

$$\mathbf{K}^{(\mathrm{e})}=S\sum_{i=1}^{M}W_i\mathbf{B}_{0i}^{\mathrm{T}}\mathbf{D}\mathbf{k}_i\mathbf{D}\mathbf{B}_{0i}\,, \tag{20}$$

3.3 Consistent mass matrix

The kinematic energy of the beam element is given by

$$\begin{aligned}
T^{(\mathrm{e})}&=\frac{1}{2}\int_0^L \rho\mathrm{A}(x)\left(\dot{u}^2+\dot{v}^2\right)\mathrm{d}x+\frac{1}{2}\int_0^L \rho\mathrm{I}(x)\left(\frac{\partial\dot{v}}{\partial x}\right)^2\mathrm{d}x\\
&=\frac{S}{2}\sum_{i=1}^{M}W_i\rho\mathrm{A}_i\left(\dot{u}_i{}^2+\dot{v}_i{}^2\right)+\frac{1}{2S}\sum_{i=1}^{M}W_i\rho\mathrm{I}_i\left(\frac{\partial\dot{v}}{\partial\xi}\Big|_{\xi=\xi_i}\right)^2
\end{aligned} \tag{21}$$

where $\rho\mathrm{A}(x)=\iint\rho(y,z)\mathrm{d}y\mathrm{d}z$ and $\rho\mathrm{I}(x)=\iint\rho(y,z)y^2\mathrm{d}y\mathrm{d}z$, respectively. The derivatives in the integral are also approximated using differential quadrature analogs. Therefore, the kinematic energy can be written as

$$T^{(\mathrm{e})}=\frac{1}{2}\dot{\mathbf{d}}^{(\mathrm{e})\mathrm{T}}\mathbf{M}^{(\mathrm{e})}\dot{\mathbf{d}}^{(\mathrm{e})}=\frac{1}{2}\dot{\mathbf{d}}^{(\mathrm{e})\mathrm{T}}\left(\mathbf{M}_0^{(\mathrm{e})}+\mathbf{M}_{\mathrm{R}}^{(\mathrm{e})}\right)\dot{\mathbf{d}}^{(\mathrm{e})} \tag{22}$$

$\mathbf{M}_0^{(\mathrm{e})}$ is the translational component of mass matrix and $\mathbf{M}_{\mathrm{R}}^{(\mathrm{e})}$ is the rotational component of mass matrix, given by

$$\mathbf{M}_0^{(e)} = S\begin{bmatrix} W_1\rho A_1\mathbf{I} & & & \mathbf{0} \\ & W_M\rho A_M\mathbf{I} & & \\ & & \ddots & \\ \mathbf{0} & & & W_{M-1}\rho A_{M-1}\mathbf{I} \end{bmatrix} \tag{23}$$

$$\mathbf{M}_{\mathrm{R}}^{(e)} = \frac{1}{S}\sum_{i=1}^{M} w_i \rho \mathrm{I}_i \mathbf{B}_{\mathrm{G}i}^{\mathrm{T}} \mathbf{B}_{\mathrm{G}i}$$

in which $\mathbf{I}$ is a 2×2 unity matrix, and $\mathbf{B}_{\mathrm{G}i}$ is a vector given by

$$\begin{aligned} \mathbf{B}_{\mathrm{G}i} &= \begin{bmatrix} \mathbf{b}_{\mathrm{G}i,2} & \mathbf{b}_{\mathrm{G}i,1} & \mathbf{b}_{\mathrm{G}i,M+1} & \mathbf{b}_{\mathrm{G}i,M+2} & \mathbf{b}_{\mathrm{G}i,3} & \cdots & \mathbf{b}_{\mathrm{G}i,M} \end{bmatrix} \\ \mathbf{b}_{\mathrm{G}i,j} &= \begin{bmatrix} 0 & G_{ij}^{(1)} \end{bmatrix} \end{aligned} \tag{24}$$

Since the numerical integration scheme and differential quadrature analog in the mass matrix formulation are consistent with those in stiffness matrix, the mass matrix in this section is still called “consistent mass matrix”.

4 ANALYSIS OF LA 3-STORY MOMENT-RESISTING FRAME

Time history analysis of a 3-story moment-resisting steel frame (Figure 3) is presented to verify the QB model. The frame is in the North-South (NS) direction, as a piece of the Los Angeles 3-story model building in the SAC steel project [13]. The material is bilinear kinematic hardening, with the elastic modulus 210, 000MPa, and the hardening modulus 6,300MPa. The yielding stress of the steel is 248MPa for all beams, and 345MPa for all columns. The distributed load on the first and second story beams is 13.90KN/m, while on the third story beams 4.57KN/m. The additional floor mass on the first and second story beams is 1,372Kg/m, while on the third story beams 915Kg/m. The mass of walls is added on the columns, which on the side columns is 1,098Kg/m and on the inner columns is 1,555Kg/m.

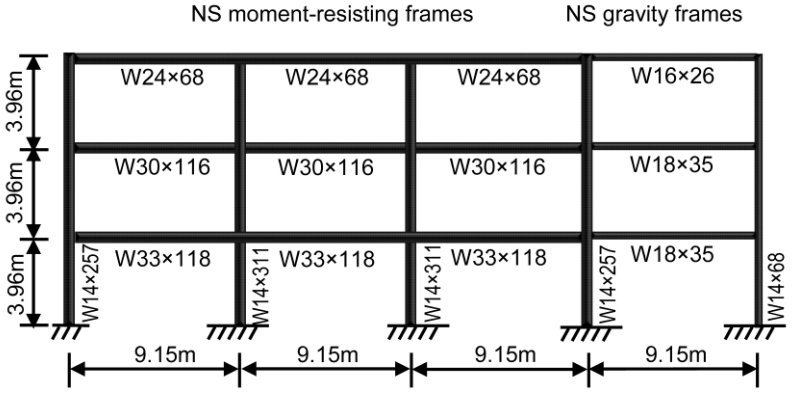

Figure 3: Elevation and member sizes of the LA 3-story Frame.

An acceleration time history of the TAFT earthquake is chosen (Figure 4) and scaled to generate ground motions with the Peak Ground Accelerations (PGAs) 0.10, 0.20, 0.30, 0.40, 0.45, 0.50 and 0.55g respectively. Time interval of the ground motions is 0.005s. Dynamic analysis of the frame is undertaken using the QB model with consistent mass matrix, coded in Fortran. To reduce the computational cost, a Guyan condensation procedure is included to condense the internal DOFs of each QB element. The characteristics of convergence and computational efficiency are studied. Dynamic analysis using the BEAM188 element with consistent mass matrix is conducted in ASNYS [16] for verification. Meantime, comparison is made with the FB beam model in OpenSEES (v2.2.0), in which only lumped mass matrix is available for inelastic dynamic analysis of frames. All computations were performed on a laptop computer with a 5-core processor @2.65GHz and 4.00G memory. The convergence criterion of Newton-Raphson iteration process is set as that the Euclid norm of residual forces is controlled to be less than 10^{-6}.

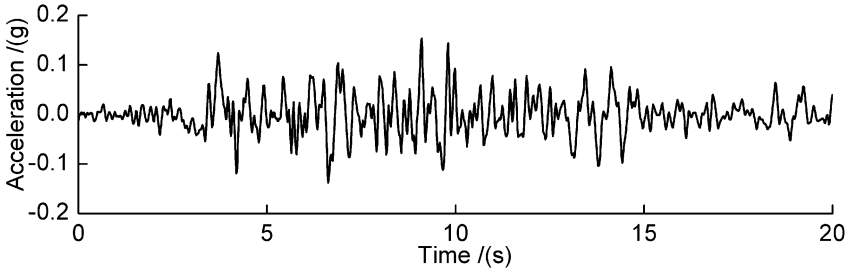

Figure 4: An acceleration time history of the TAFT earthquake.

Figures 5 and 6 show the displacement responses and acceleration responses at the roof for the three models. In QB and FB models, the number of integration points in one element is chosen as M = 10. In ANSYS, 10 four-node BEAM188 elements are used to simulate one frame member, and shear deformation is adjusted to be negligible. The QB results agree with ANSYS results, and are slightly different from the FB results in OpenSEES.

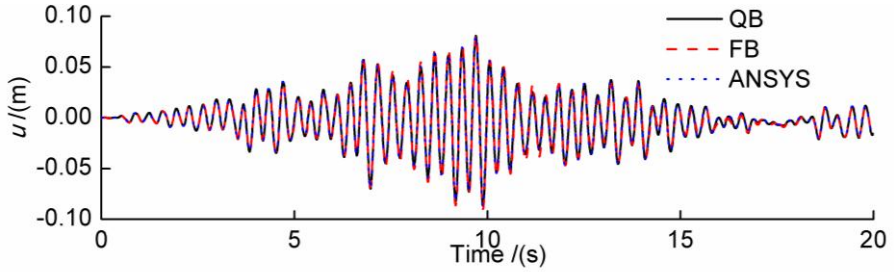

Figure 5: Time histories of the roof displacement responses for the three models, PGA=0.50g.

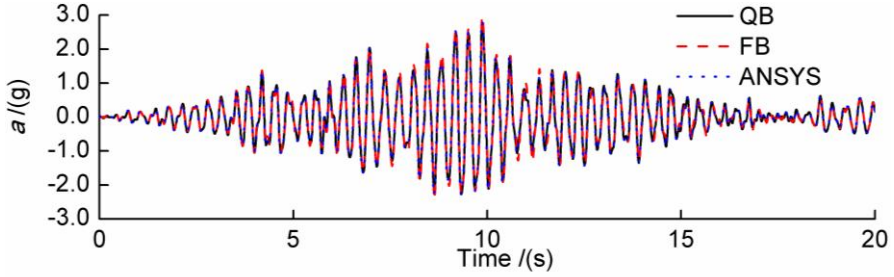

Figure 6: Time histories of the roof acceleration responses for the three models, PGA=0.50g.

The peak values of the responses are illustrated in Figures 7 and 8. Referring to the ANSYS results, the QB model is accurate in the inelastic dynamic analysis. The FB results have relative errors about 5% to 10%. It is believed that the lumped mass matrix of the FB model reduces the accuracy.

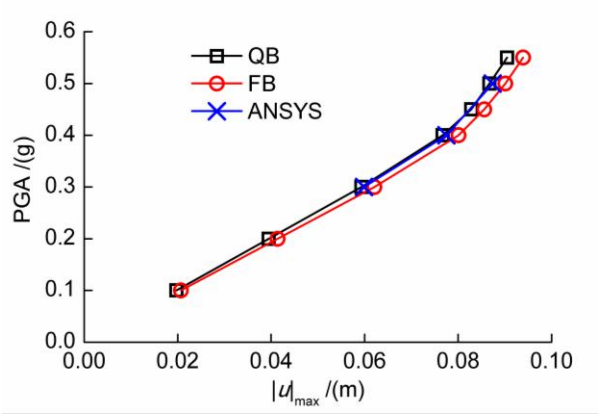

Figure 7: Peak values of the roof displacement responses for different PGAs.

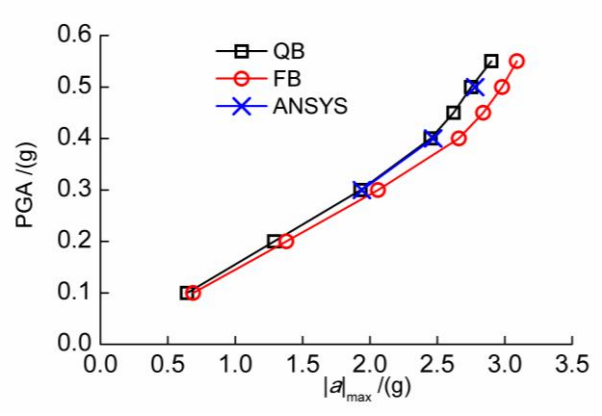

Figure 8: Peak values of the roof acceleration responses for different PGAs.

Figure 9 gives the convergence of the peak response $|u|_{max}$ of the QB and FB models under PGA=0.50g for different number of integration points *M*. In OpenSEES, *M* is restricted to be not greater than 10. Results of both models can converge by increasing *M*, and their convergence rates are similar.

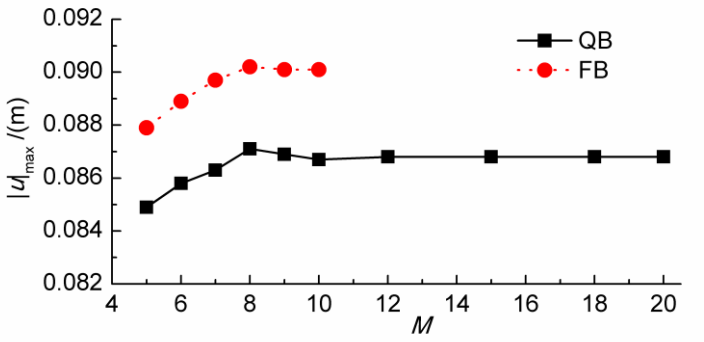

Figure 9: Peak values of the roof displacement responses for different *M*, PGA = 0.50g.

The CPU time consumptions of the three models are listed in the Tables 1 and 2. The commercial code ANSYS is versatile and accurate, but its computational cost is much greater for seismic analysis of an entire structure. The computational cost of the QB model is close to that of the FB model in OpenSEES. When increasing the number of integration points *M*, the CPU time consumption of the QB model increases almost linearly. The quadrature beam model is efficient and suitable for seismic analysis of frames.

PGA /(g)	t_{QB} /(s)	$t_{OpenSEES}$ /(s)	t_{ANSYS} /(h)
0.10	40.0	33.5	—
0.20	40.1	33.6	—
0.30	40.3	33.2	12.5
0.40	47.9	33.8	13.0

0.45	49.4	34.8	—
0.50	54.2	35.5	13.5
0.55	59.8	36.0	—

Table 1: CPU time consumptions for different PGAs.

M	t_{QB} /(s)	$t_{OpenSEES}$ /(s)
5	25.1	18.2
6	31.8	21.5
7	35.5	24.5
8	41.4	27.2
9	48.9	30.8
10	54.2	35.5
15	83.5	—
20	120.5	—

Table 2: CPU time consumptions for different M.

5 CONCLUSIONS

- A distributed-plasticity quadrature beam (QB) model with consistent mass matrix is formulated in this paper. For inelastic dynamic seismic analysis of frames, one member is simulated by one QB element.
- The accuracy and the convergence of the QB model are verified. Results of the QB model are in excellent agreement with those of the DB model in ANSYS, but the CPU time consumption is much lower. The convergence rates of the QB and the FB models are comparable, and the time consumption of the QB model is slightly higher. In contrast to the only available lumped mass matrix of the FB model, however, the consistent mass matrix of the QB model makes it advantageous for inelastic dynamic analysis.
- The quadrature beam model is accurate and efficient, highlighting its great potentials in seismic analysis of frames.

ACKNOWLEDGEMENT

This present work was undertaken under the support of the National Natural Science Foundation of China (No. 50778104) and China Postdoctoral Science Foundation (No. 20100480320).

REFERENCES

[1] M. Ohsaki, T. Miyamura and M. Kohiyama *et al*, High-precision finite element analysis of elasto-plastic dynamic responses of super-high-rise steel frames. *Earthquake Engineering & Structural Dynamics*, **38**(5), 635-654, 2009.

[2] D.W. White, Plastic hinge methods for advanced analysis of steel frames. *Journal of Construction Steel Research*, **24**(2), 121–52, 1993.

[3] A. R. Mari, A. C. Scordelis, Nonlinear geometric, material and time dependent analysis of three-dimensional reinforced and prestressed concrete frames. *Report UCB/SESM-84/12*, U. C. Berkeley, 1984.

[4] B. A. Izzuddin, A. Siyam, Smith D L, An efficient beam-column formulation for 3D reinforced concrete frames. *Computers & Structures*, **80**, 659-676, 2002.

[5] P. Šolín, K. Segeth, I. Doležel, *Higher-order finite element methods*. Chapman & Hall/CRC, USA, 2003.

[6] S. Mazzoni, F. McKenna, M. H. Scott, G. L. Fenves, *OPENSEES user's manual*. PEER, U. C. Berkeley, 2007.

[7] V. Ciampi, L. Carlesimo, A nonlinear beam element for seismic analysis of structures. *8th European Conference on Earthquake Engineering*, Laboratorio Nacional de Engenharia Civil, Lisbon, 1986.

[8] E. Spacone, F. C. Filippou, F. F. Taucer, Fibre beam-column model for non-linear analysis of R/C frames: part I. Formulation. *Earthquake Engineering & Structural Dynamics*, **25**(7), 711–725, 1996.

[9] A. Neuenhofer, F. C. Filippou, Geometrically nonlinear force-based frame finite element. *Journal of Structural Engineering ASCE*, **124**(6), 704-711, 1998.

[10] C. Molins, P. Roca, A. H. Barbat, Force-based linear dynamic analysis of complex structures with curved-3d beams. *Earthquake Engineering and Structural Dynamics*, **27**, 731-747, 1998.

[11] H. Zhong, M. Gao, Quadrature element analysis of planar frameworks. *Archive of Applied Mechanics*, **80**, 1391-1405, 2010.

[12] H. Zhong, Y. Wang, Weak form quadrature element analysis of Bickford beams. *European Journal of Mechanics A/Solids*, **29** (5), 851-858, 2010.

[13] FEMA-355C. *State of the art report on systems performance of steel moment frames subjected to earthquake ground shaking*. Federal Emergency Management Agency, 2000.

[14] R. E. Bellman, J. Casti, Differential quadrature and long term integration. *Journal of Mathematical Analysis and Applications*, **34**, 235-238, 1971.

[15] P. I. Davis, P. Rabinowitz, *Methods of Numerical Integration (2nd edition)*. Academic Press, Orlando, 1984.

[16] *ANSYS User's Manual, Version 8.0,* Swanson Analysis Systems Inc. (SASI), Houston, PA, 2004.